



Rotational speeds and preheating Effect on the friction stir butt welding of Al-Cu joints



CrossMark

H. I. Dawood¹; Abbas Khalaf Mohammad¹; Kanaan Mohammad Musa¹, Nawras Shareef Sabeeh²

¹Department of Chemical Engineering, College of Engineering, University of AL-Qadisiyah, AL- Qadisiyah, IRAQ

²Department of Mechanical Engineering, College of Engineering, University of AL-Qadisiyah, AL-Qadisiyah, IRAQ

Abstract

Friction Stir Welding (FSW) used for welding similar and dissimilar materials especially to join sheet Al alloys. In this study, commercial pure aluminum and copper sheets (Al/Cu) with a thickness of 3mm were joined. We first preheated on the Cu side by pinless welding tool. Three different tool rotational speeds of 700, 1000 and 1500 rpm were used while the axial load and transverse speed were kept constant at 7.5 KN and 30 mm/min, respectively. We measured different parameters to determine the best rotational speeds for welding. Such as Field Emission Scanning Electron Microscopy (FESEM) and X-Ray Diffraction (XRD) analysis which showed that at 700 rpm there are three elements: Al, Cu and oxygen are present. While at 1500 rpm formation of different Intermetallic Compounds (IMCs). At 1000 rpm the interface has only Al and Cu in a uniform structure this result is due to the sufficient frictional heat generated at 1000 rpm and it considered perfect welds with acceptable mechanical properties.

Keywords: Friction stir welding, Dissimilar Al-Cu joints, Nugget zone, Rotational speed, Intermetallic compounds, Thermal expansion coefficient.

1- Introduction

Friction Stir Welding (FSW) has shown great potential to join similar and dissimilar materials[1-3]. It is a solid-state joining process introduced by The Welding Institute in 1991[4]. FSW join two facing workpieces without melting the workpiece material [5, 6]. A non-consumable rotating tool was produced frictional heat, plastic deformation of the metal contact occurs, leading to mixing the workpiece materials. They have advantages over conventional joining techniques used to produce joints[7-9]. Such as FSW don't have porosity, cracks and distortion during the application[10, 11]. Recently, there are many studies on joining dissimilar materials[12, 13]. The accurate joining of dissimilar materials is used in many fields including the nuclear, chemical, transportation, power generation, aerospace and electronics industries.[14-16]. By using FSW can obtain Al Cu weld joint. Aluminium and copper have excellent electrical and thermal conductivities they are widely applied in various applications, primarily in electrical, automotive, and refrigeration industries [8, 17]. From the application of FSW in industries that use aluminum are shipbuilding, aerospace, railroad and automotive industry. Al Cu joint by

FSW observed an excellent metallurgical bond, improved its hardness and strengthened the weld joint [17].

Aluminium and copper dissimilar joints is often used in many applications, for example batteries tab to busbars joining, transformer foil conductors, condenser, electrical connectors, capacitor foil windings, heat exchanger tubing, refrigeration tubes, and tube covers[18, 19] . So in this article we studied FSW for Al Cu, Cu is a harder material than Al; so firstly the preheating was conducted on the Cu side by a pinless tool. FSW for Al and Cu occurred at three rotating speed (700, 1000 and 1500 rpm) to produce perfect welds with acceptable mechanical properties.

2- Materials and experimental procedures

2.1 Materials

Cu and Al sheets 3 mm thick were bonded by FSW. The sheets were cut into pieces with dimensions of 100mm × 75mm. The pieces were ground with grit paper to remove the oxide layer and then cleaned with acetone to form a better joint. Before welding, the plates were placed on a supporting plate and firmly fixed by an anvil along the welding direction

*Corresponding author e-mail: hasan.dawwood@qu.edu.iq; (H. I. Dawood).

EJCHEM use only: Receive Date: 06 December 2021, Revise Date: 23 December 2021, Accept Date: 26 December 2021

DOI: [10.21608/ejchem.2021.109836.5007](https://doi.org/10.21608/ejchem.2021.109836.5007)

©2022 National Information and Documentation Center (NIDOC)

to prevent relative movement. A welding tool of medium carbon steel with a shoulder of 16mm in diameter, a pin of 4mm in diameter and 2.7mm in length was heat-treated to a hardness of 58HRC. The

chemical compositions of the experimental materials (Al, Cu and medium carbon steel) are listed in Table 1 [25].

Table 1. Chemical compositions of the pure Al, pure Cu and medium carbon steel (wt %)

Material	Al	Si	Fe	Mg	Cu	Mn	Pb	C	P
Pure Al	Balance	0.114	0.405	0.032	0.08	0.011	-	-	-
Pure Cu	-	0.0039	0.013	-	Balance	-	0.02	-	-
Medium carbon steel	-	-	Balance	-	-	0.79	-	0.44	0.012

2.2 Friction stir welding process

The process of FSW was carried out using KAMA milling machine (X6325, 3Hp, TRPER R8, 30 KN). The milling machine head is set at a rotating speed of 700, 1000 and 1500 rpm, and a transverse speed of 30 mm/min. The axial load was kept constant at 7.5 KN through the process of welding. The connecting surface of commercial pure Al and Cu was cleaned with acetone liquid before starting the welding process to remove stains and grease that affecting welding quality, and then ultrasonic cleaned to remove impurities. In this welding process, the side where the velocity vector of the rotating tool and transverse speed are in the same direction refers to Advancing Side (AS); while the side opposite to velocity vectors indicates to Retreating Side (RS) as shown the schematic diagram in Fig. 1. Cu, is a harder material, was fixed at the AS; while Al fixed at RS as it had a lower melting point than Cu. The pure Cu plate was fixed on the AS and the Al plate was fixed on the RS in order to facilitate sufficient material flow during the welding process. Moreover, preheating was conducted on Cu side using a pinless welding tool. For the welding process, unthreaded columnar pin and smooth shoulder were used. The tool tilt angle was 4° , and the tool pin had a constant offset about 1mm towards the Al side in order to improve joint forming structure, material flow and welding quality.

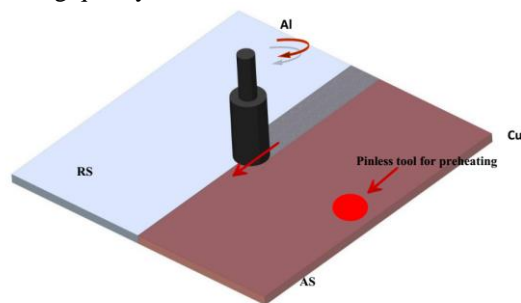


Figure 1. Schematic diagram of an dissimilar FSW for Al-Cu.

2.3 Temperature measurements

The temperature during the FSW process was measured by K-type thermocouples fixed to the

Al and Cu surfaces at different distances closed to the shoulder boundary. The temperature measurements were implemented using a digital thermometer (Ebro TFN 520/530, Produktions-u. Vertriebs GmbH, Germany) based on the standard DIN IEC 584-2 for accuracy of the probe. It was observed, the temperature increased rapidly until it reached the maximum level. The main goal for this article to find the effect of temperature on the welding parameters and the microstructure at the interface.

2.4 Material Characterization

Typical photographs of the welded joints at different rotational speeds were carried out using (SM: N900). For interface analysis, the specifications of the cutting, grinding and polishing were performed according to the ASTM: E3 standards. All samples were ground by rubbing abrasive grit papers (200-1500), then polished with $2\mu\text{m}$ alumina paste as final polish and cleaned in an acetone bath. The Al side was etched chemically using a sodium hydroxide solution (1%NaOH) for 15min. After that, the Cu side was etched with a solution of 10g ammonium persulfate and 100ml distilled water to reveal the microstructure at the interface. Microstructure of the specimens were observed using (ZEISS SUPRA35VP) FESEM. Energy Dispersive X-ray (EDX) analysis was also performed to scan the formed of delicate structure in the NZ. Thermal expansion coefficient at the interface of welded joints was investigated using Linseis, L50. The welded joints interfaces were examined by XRD, using a copper target to distinguish the phases formed. For this purpose, the instrument of D8 Advance X-ray diffractometer (Bruker Analytical X-Ray Systems) was used. The average Vickers test of microhardness over normal cross-section of the weld was measured according to ASTM: E384 standards, using (FV-700E). Tensile tests were also performed using INSTRON-5569P7531 (Universal Testing Machine) operating at 1mm/min in accordance with ASTM: E8 standards references. Finally, the FESEM test was also used to examine the tensile fracture surfaces of the specimens.

2.5 Frictional heat input during FSW

FSW tool is a key process parameter whose task is to provide adequate heating and softening to the workpiece due to the friction that occurs between the tool and the workpiece. It also provides proper movement of the deformed material, extrudes the base materials around the tool in the vertical and horizontal direction, and finally the solid state joining of the material occurs[20]. FSW tool has an effect on the thermal heat input, plastic material flow, strength, and torque encountered through joining of base materials; therefore, it must be carefully selected and designed[21]. The tool shoulder diameter is one of the important parameters of FSW for defect-free connection with good quality and should be selected accurately. The shoulder of the tool has two basic roles because it incites the axial force down and also holds the main part of the friction heat. Heat generation and resulting extreme temperature developments are greatly influenced by shoulder diameter and rotational speed during FSW [8, 22]. It has been reported that about 87% of the frictional heat generated by the frictional motion between the workpiece and the shoulder surface is subscribed by the diameter of the tool shoulder [23]. Insufficient heat breaks the pin part of the tool as it does not provide sufficient softening in the material [17]. The shoulder of the tool also plays an important role in forging the stirred material. During the dissimilar FSW of Al-Cu, the microstructure, mechanical properties, deformation of materials, IMCs formation and change of diving load are affected by tool type and tool rotation speed.

In the FSW process, heat is generated by friction and transmitted to both the tool and the work piece. Factors such as the amount of heat transferred to the work piece, the weld shape, the weld quality, the weld microstructure, the formation of residual stress, the deformation in the work piece, also determine the success of the FSW process[17].

3. Results and discussion

3.1 Characterization of temperature and heat flux in relation to rotational speeds

Friction Stir welding (FSW) process used to raise the temperature near the weld line boundary by frictional heat produced by a non consumable rotating tool, plastic deformation of the metal contact occurs, leading to mixing the work piece materials [24].

In this article we constant the friction coefficient μ and normal load so the thermal conductivity depends on rotational speed and the nature of intended materials for welding.

The average heat input and the resulting heat flux can be calculated by the following correlations [25];

$$q_o = \frac{4}{3} \pi^2 \mu P N R^3 \dots (1) \quad \text{And}$$

$$Q = \frac{q_o}{A_C} \dots (2)$$

Where q_o is the heat input, μ is the friction coefficient and was assumed constant during FSW process, P is the pressure distribution across the interface, N is the rotational speed, R is the shoulder radius, Q is the heat flux and $A_C (R^2 \times \pi)$ is the contact area.

From Fig. 2 we concluded that the best welding specimen are occurred at temperature 485°C under rotational speed of 1000 rpm and temperature for welding Al-Cu is 254°C at rotational speed of 700 rpm. Cu has higher thermal conductivity than Al metal so at higher rotational speed of 1500 rpm a higher temperature (627°C) is recorded.

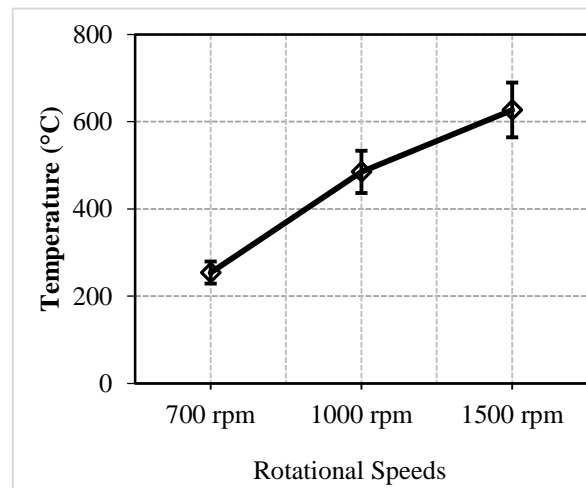


Figure 2. Effects of rotational speeds on the frictional temperature for joining commercially available pure Al and Cu.

From Fig:3 shown that by the highest rotational speed (1500 rpm) the highest heat flux are produced, vice versa.[26] Form the results we can observed that the rotational speed is reduced from 1500 rpm to 700 rpm, frictional heat flux is reduced by about two times which agree with the survey[26].

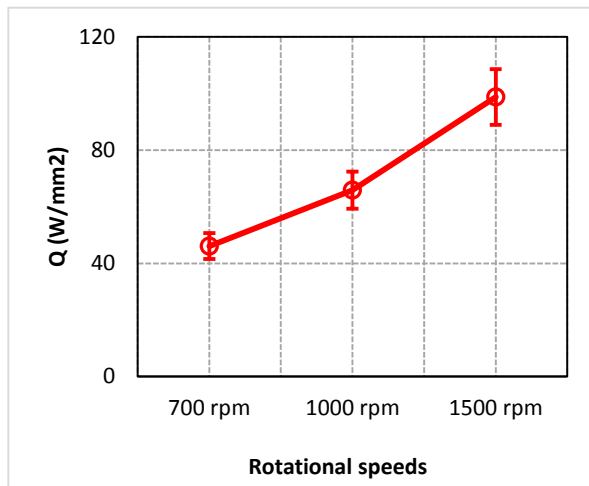


Figure 3. Effects of rotational speeds on the frictional heat flux for joining commercially available pure Al and Cu.

3.2 Selection of an appropriate heat input

It is very important factor which determines the best rotational speeds creates an appropriate temperature from frictional for welding. Cu is a harder material than Al; so firstly the preheating was conducted on the Cu side by a pinless tool then studied the the best FSW of Al-Cu under three rotational speeds. From fig. 4(b) we concluded that the best FSW of Al-Cu at 1000 rpm, the surface is rough due to spread Cu in Al, and forming a homogeneous mixing of the materials during welding process [27]. The phenomenon of thermal heat generation in welding is judged to aid in grain coarsening and cause the observed increase in average grain sizes [28]. Fig. 4(a) showed the joint surface of Al-Cu, using the rotational speed of 700 rpm. The figure did not show agreement of a suitable welding parameter[25]. During FSW process the flash of the welding was gathered beside the welding line and grooves and voids are observed. Probably, heat input from the rotational speed of 700 rpm was not enough to welding or due to the poor interaction between the pin tool and the work pieces [29-31].

As seen in Fig. 4(c), at the rotational speed of 1500 rpm, cracks and voids can be seen along the interface between Base Metals (BMs). This result may come from the excessive heat input due to a higher rotational speed and preheating on Cu side. Hence, it can be concluded that the appropriate parameters such as rotational speed with preheating can yield a good quality of the joined surfaces (i.e. appropriate heat input) [32].

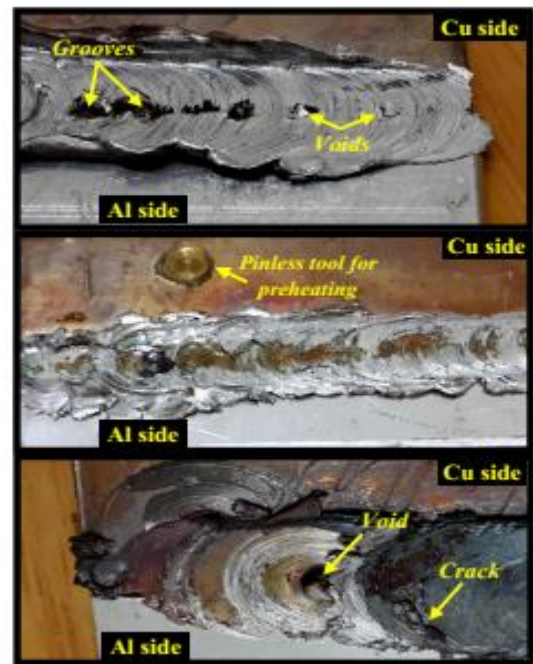


Figure 4. Typical photographs of dissimilar commercially available pure Al and Cu FSW at different rotational speeds; (a) 700 rpm and (c) 1500 rpm.

3.3 FESEM and EDX analysis of FSW joints at the interface

Emission Scanning Electron Microscopy FESEM of FSW for Al-Cu sample Fig. 5(a), show that at arotational speed of 700 rpm the interface between Al-Cu has a gap, crack and bonded together by weakly forces. These defects are due to the frictional heat generated at 700 rpm that is insufficient to deform the Cu sufficiently at the interface. Fig. 5(b) shows a magnified view of the surrounded region in Fig. 5(a)

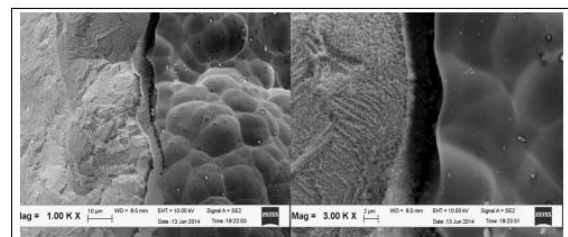


Figure 5. Interface between Al-Cu observed under FESEM at 700 rpm: (a) 1000X and (b) 3000X.

Energy Dispersive X-Ray (EDX) analysis is a technique used to identify the elemental composition of materials. When EDX used for interface area in joint at 700 rpm as appeared in fig. 6. There are three elements: Al, Cu and oxygen. The high percentage of oxygen content is due to

relative oxidation coincided. EDX analysis shows the ratio of Al atoms to Cu by about 2.7. Al and Cu are only observed in the fabricated joint at 700 rpm but during the reaction Cu and Al there are different Intermetallic Compounds IMCs are formed such as $(Al_2Cu, AlCu, Al_3Cu_4 \text{ and } Al_4Cu_9)$ [30, 33, 34].

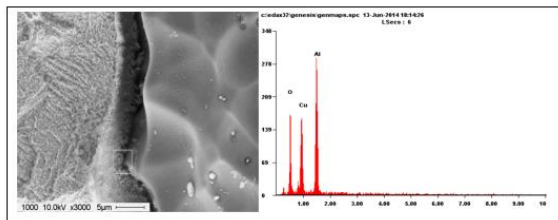


Figure 6. EDX analysis of dissimilar Al-Cu at the interface, FSW at 700 rpm.

Fig. 7 shows the FSW interface of dissimilar Al and Cu at rotational speed of 1000 rpm. As seen in Fig. 7(a), the interface between Al and Cu has a uniform structure. Probably, this result is due to the sufficient frictional heat generated at 1000 rpm. The structure of interfaced between Al and Cu shows the firm bond in this region. The bright side refers to Cu and the dim side refers to Al. The magnified view at the interface between Al and Cu is shown in Fig. 7(b); A sharp edge between Cu BM and the NZ can be noticed; while the edge at Al BM is indistinguishable. So at the best FSW of Al-Cu 1000 rpm

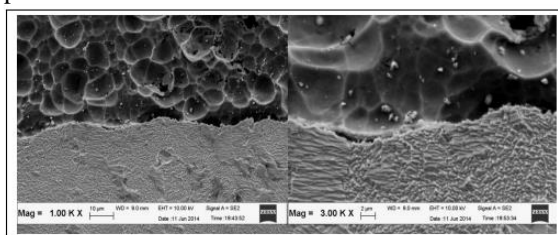


Figure 7. Interface between Al-Cu observed under FESEM at 1000 rpm: (a) 1000X and (b)3000X.

Fig. 8 shows the EDX analysis of a butt joint interface that friction stir welded at 1000 rpm. The figure shows that the bonded area consists of Al, Cu and small percentages of oxygen due to the oxidation. However, the wt% of Mg and Si may come from deep impurities of the BMs. The FSW of dissimilar metals can be clearly recognized from the weldings of similar metals through the formation of complex compound and related materials flow [35, 36].

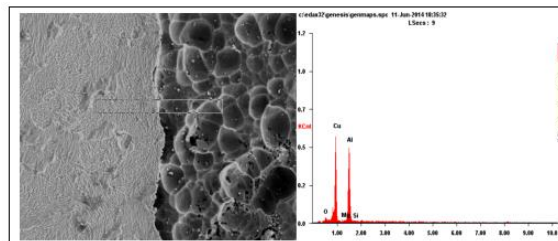


Figure 8. EDX analysis of dissimilar Al-Cu at the interface, FSW at 1000 rpm.

In Figs. 9(a) and 9(b), swirl patterns and streamlines at the interface can be seen clearly. It indicates that a strong plastic deformation has occurred through FSW process at a higher (1500 rpm) rotational speed. In the stir zone, the white lamellar structure is composed of Cu particles of streamlines shape and continuous allines can be observed (i.e. IMCs). However, many of IMCs exist in the interface between Al and Cu due to the excess of frictional heat input [37, 38].

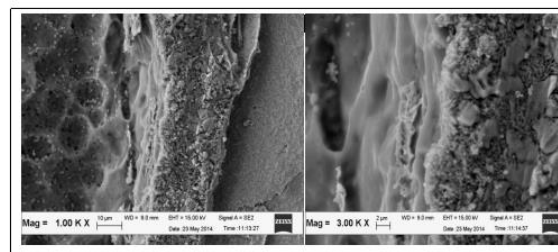


Figure 9. Interface between Al-Cu observed under FESEM at 1500 rpm: (a) 1000X and (b) 3000X.

Fig. 10 shows the EDX at interface between Al and Cu that friction stir welded at 1500rpm. By increasing the rotational speed there are many IMCs formed during welding process, such as Al_2Cu and Al_4Cu_9 .

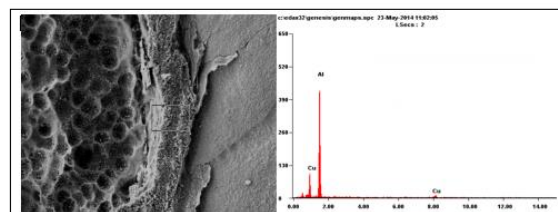


Figure 10. EDX analysis of dissimilar Al-Cu at the interface, FSW at 1500 rpm.

3.4 Thermal expansion of BMs and interface of the welded joints

Along the interface of Al-Cu joint, the thermal stresses were irregular which is focused on the whole joint. Another reason for stress generation, the structure of flash that formed beside the welded joint; the longitudinal stresses turn into tensile stresses between the deformed and non-deformed materials[39]. Tensile stress at the interface that caused by the thermal stresses is considered the most harmful effect. Since the stress axis is perpendicular

to the welding line, so it reduces the joint strength. The magnitude of residual stress depends on the welding dimensions in the facing area.

A larger deformed of the welding area leads to a larger residual stress production. Hence, the strength is decreased when a joint with large thermal expansion (i.e. large residual stress). Nevertheless, it rarely occurs when some of specimens are strong in bonding and some are weak even they belong to the same group. This phenomenon is due to the internal distribution of material flaws and accompaniment thermal stresses during the process of joining [21, 26].

The mismatch in thermal expansion between Al-Cu is one of the main issues in joining. Generally, the thermal expansion coefficient of Cu is lower than Al. Fig.11 illustrates the thermal expansion coefficient and its relationship with the temperature for commercially pure Al and Cu BMs. The thermal expansion between the BMs shows variation in the curves. Up to 320°K, Cu and Al BMs show the match of thermal expansion, followed with a considerable difference between 400 and 700 °K.

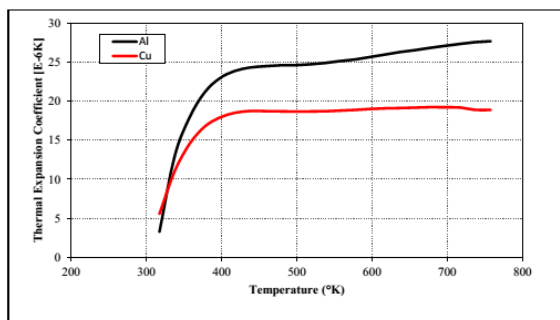


Figure 11. Thermal expansion coefficient versus temperature for dissimilar commercially available pure Al and Cu BMs.

Fig. 12 shows the thermal expansion coefficient versus the interface temperature of the welded joints at different rotational speeds. below 400 °K, the thermal expansion matches at the interface between the fabricated joints at 1000 rpm and 1500 rpm as compared to the joint interface that fabricated at 700 rpm. However, beyond 320 °K, the curves of both welded joints interfaces (1000 rpm and 1500 rpm) are increased dramatically and their ascent is higher than the welded joint at 700 rpm. Between 600°K and 700°K the thermal expansion curves for joints and interfaces that welded at 700 rpm and 1500 rpm fitted very well. Hence, it could be concluded that the distribution of Al and Cu particles along the interface is not uniform; and also means that the specimens have different thermal expansion coefficients for the same joint at the interface. However, the interfacial structures of welded joints and the BMs are indistinguishable, and the mismatched features of expansion causes the variance

in residual stresses. In addition, it is a testament to the grains expansion in the welding area near Cu. As previously mentioned, the Cu BM has a lower thermal expansion coefficient than the Al BM. Accordingly, it can be concluded that a high expansion of thermal coefficient is due to the existence of a high percentage of Al, and a low expansion of thermal coefficient is due to the existence of a high percentage of Cu.

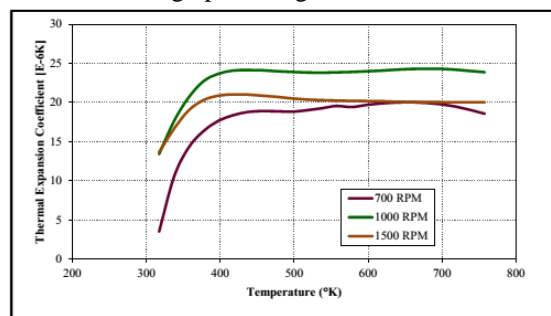


Figure 12. Thermal expansion coefficient versus temperature for dissimilar commercially available pure Al-Cu welded joints at the interface with different rotational speeds.

3.5 X-ray diffraction (XRD) analysis

Commercial Al-Cu joints were analyzed by XRD spectrum, using a copper target. The appropriate parameters related to the diagram of diffraction peaks were calculated using X' Pert High Score Plus software which indicates that Al-Cu is a cubic structure. The analysis results of XRD are shown in Fig.13a at 700 rpm only Al and Cu appear in the joint and no IMCs (there are not reaction occur between Al and Cu during FSW), [40] fig. 13b, shown that when the rotational speed increase to 1000 rpm a small amount from (Al₄Cu₉) appeared which indicate that the the beginning reaction between Cu and Al. On the other hand Al₂Cu and Al₄Cu₉ are produced by increase rotational speed to 1500 rpm fig.13c. This explains that by increase the temperature the solid state reaction occur between Cu and Al[41]. According to the findings of some studies, during Al-Cu reaction, Al-Cu rich phases which were formed the first two IMCs close to Al and Cu sides, respectively [42, 43]. Therefore, the sub-layer nearby the Cu should be Al₄Cu₉ and nearby Al should be Al₂Cu.

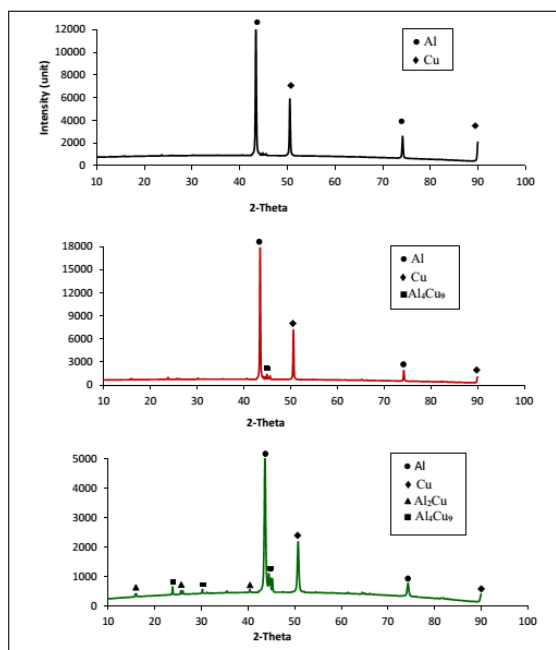


Figure 13. X-ray diffraction analysis of the fabricated joints at (a) 700 rpm, (b) 1000 rpm and (c) 1500 rpm.

The XRD data (Table 2) shows the changes in metal density, crystallite size and lattice parameters that occurred at the FSW joints with different rotational speeds. The comparison of the computed results with the relevant parameters of the BMs matched with the reference code 98-004-8848 and 98-008-7417, respectively.

Table 2 XRD results of commercial pure Al and Cu BMs and the FSW joints at different rotational speeds near the interface

Relevant parameters	Al BM	Cu BM	Welded joints at different rotational speeds (rpm)		
			700	1000	1500
Density (calculated) (gm/cm ³)	2.6795	8.9928	5.4094	5.4091	5.2241
Crystallite size (nm)	64.87	55.35	74.7	101.72	73.49
Lattice parameters (a, b, c) °A	4.059	3.607	12.07	12.066	12.137

The obtained results from Table 2 showed many differences; these differences indicate that during FSW experiments the crystallite size was influenced. XRD results were compared with BMs, to identify differences in XRD assessment of crystallite size using Scherrer method. Comparing the initial X-ray density in the BMs with the FSW joints at different rotational speeds, a slight decrease of the X-ray density was recorded. During plastic deformation, the strain hardening behavior associated with different rotational speeds can be influenced by the crystallite size and lattice parameters of the granular structure [44]. Transient microstructure observation is an important factor as it helps to understanding the complex FSW process at changeable rotational speeds which includes the deformation and dynamic recrystallization.

3.6 Mechanical properties

3.6.1 Vickers Microhardness measurements

Representative cross-section of Vickers micro hardness profiles of dissimilar welds was measured along the dashed lines specified in figure 14. The microhardness of the Cu side is obviously higher than that of the Al side. The highest microhardness is found in the NZ region near the Cu side, which is higher than the BM of Cu. This may be due to solid solution strengthening and grain refinement. XUE et al [45] also found that the

microhardness in this region was higher than that in the other region, due to the high proportion of IMCs. Since there are no IMCs in the welded specimen at a rotation speed of 700 rpm and low microhardness is due to a lack of thermal heat inputs resulting in inefficient mixing of materials with increasing defects in the stirring area. The microhardness values in the NZ welding area that created at a rotation speed of 1000 rpm showed a higher value than the Thermo-Mechanical Affected Zone (TMAZ), Heat-Affected Zone (HAZ) and BMs. This behavior may be attributed to reduce in grain size according to the known Hall-Petch relationship [46]. Indeed, besides grain size, there are many factors that affect the microhardness of FSW for hybrid materials. The main reasons that leading to high microhardness can be summarized as follows; the presence of large Cu particles and high dislocation density [32, 47].

From the results of the microhardness in figure 14 (discontinuity in the microhardness due to voids), it is noted that high values of microhardness are achieved in the welding line at NZ for all three specimens. It is a clear indication that a large mixed area is forming under the affected region (tool shoulder). Furthermore, the very high microhardness values of HV ~ 375.4 shown in the specimen that fabricated at 1500 rpm parameter which indicated the formation of fragile IMCs in those areas.

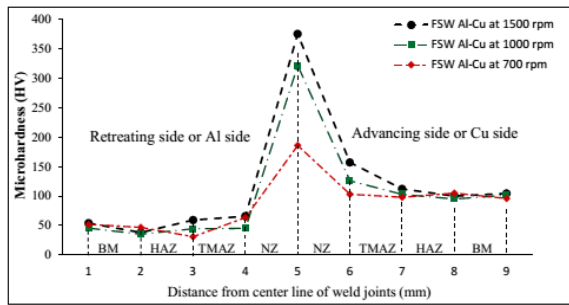


Figure 14. The average Vickers microhardness was measured on the cross-section of dissimilar Al-Cu welds at different rotational speeds.

3.6.2 Tensile strength

Fig. 15 shows the tensile profile of the welded joints at rotational speeds of 700 rpm, 1000 rpm and 1500 rpm. Which show that the tensile strength of the welded joint with a rotational speed of 1000 rpm higher than that of the welded joints with rotational speeds of 700 rpm and 1500 rpm. So the strength of the dissimilar friction stir welded joint at 1000 rpm is relatively very well. The lower tensile strength at 1500 rpm attributed to the created of IMCs such as Al_2Cu and Al_4Cu_9 . Furthermore, most welded joints were fractured on the Al side (TMAZ) near the NZ, because the materials structure in the NZ subjected to severe plastic deformation, so it produced a fine grains if comparison to TMAZ, and consequently leads to a high microhardness and tensile strength (Hall-Petch equation). It is known that, the tensile strength of Al is lower than Cu BM; therefore, most of the welded joints were broken by Al side. This fact in full agreement with Li et al. [40]. According to the results in Fig. 15, the fabricated joints at rotation speeds of 700 rpm and 1500 rpm from TMAZ were fractured from Al side; while the fabricated joint at rotational speed of 1000 rpm was fractured from NZ. As mentioned earlier, this study was carried out to find the acceptable rate of heat input with the help of preheating on Cu side to achieve the best welding properties. Hence, it can be inferred, that the fabricated joint at rotational speed of 1000 rpm considered the best parameter in our search, because under this parameter, high tensile strength was achieved without defects.

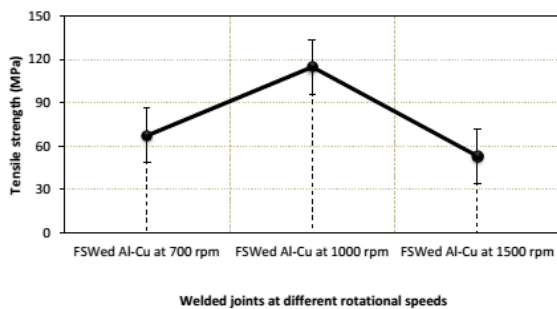


Figure 15. Tensile profile for welded joints with rotational speeds of 700 rpm, 1000 rpm and 1500 rpm.

3.7 Fractography

Using FESEM, studied fractographs were captured on the areas of tensile fracture specimens to understand of the failure mechanism of the friction welded joint, From Fig.16a we concluded that the tensile fracture of friction stir welded joint at 700 rpm. The fracture features indicate that the break area occurred near NZ by Al side. Micro cracks and voids could be seen at some fracture regions by Al side which indicate that this region is relatively weak. (Fig. 16c) showed that at rotational speed of 1000 rpm formed a ductile fracture case as well as some of dimples was observed at different depths, indicating that the fracture area is ductile. [48] find out the presence of fine and homogeneous microscopic grains in the broken area which led to formation of small dimples. (Fig. 16e) at rotational speed of 1500 rpm brittle fractures and cracks were observed in the fabricated joint. The figure shows an uneven surface; and complex microstructures at the NZ. The features of fracture surface in the friction stir welded joint at 1500 rpm show all parts exhibit a typical brittle fracture mode with some cracks. Hence, the exact nature of this fracture is a ductile and brittle. of Crack growth is usually caused by a large dimple due to its coarser surfaces that have greater plastic deformation and ridge features [49].

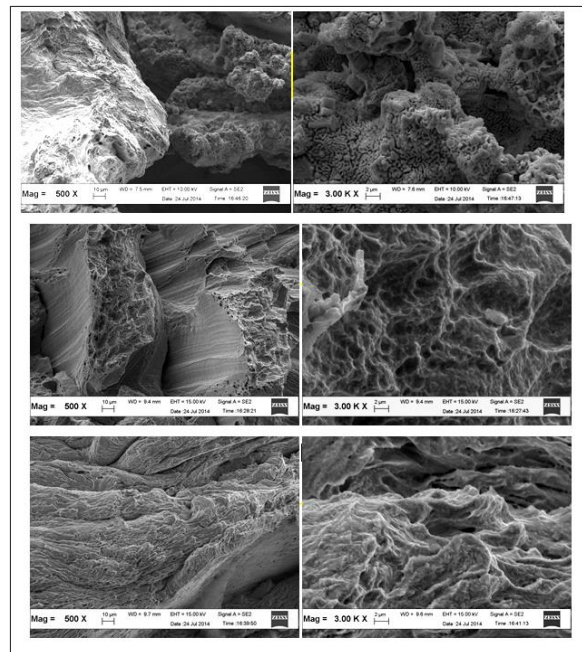


Figure 16. FESEM images showing tensile fracture surface mode of dissimilar Al-Cu joints; (a) The

FSW joint at 700 rpm, 1000x and (b) at 3000x; (c) The FSW joint at 1000 rpm, 1000x and (d) at 3000x and (e) the FSW joint at 1500 rpm, 1000x and (f) at 3000x.

4. Conclusions

By using FSW, welding of Al and Cu was successfully performed. The appropriate parameters such as rotational speed with preheating can get a good weld quality. We studied Al and Cu joint under three rotational speed to get different friction temperature and studied the different parameters to detect the best rotational speed for welding. At 700 rpm, the joint surface of Al-Cu does not have unanimous agreement of a suitable welding parameter and it has a gap, crack and bonded together by weakly forces, at 1500 rpm there are cracks and voids along the interface between base metals while at 1000 rpm the surface morphology is rough and there is no more flash existence. X-Ray Diffraction (XRD) analysis showed that at 700 rpm only Al and Cu appear in the joint and no IMCs (there are not reaction occur between Al and Cu during FSW), the rotational speed increase to 1000 rpm a small amount from (Al₄Cu₉) appeared which indicate that the the beginning reaction between Cu and Al and at 1500 rpm Al₂Cu and Al₄Cu₉ are produced. When mismatch in thermal expansion coefficient between the metals decreased the strength and this effect depends on the presence of internal flaw induced by thermal stress. The distribution of Al-Cu along the interface is not uniform; therefore each specimen have different expansion coefficient. High Al percentage lead to a high thermal expansion coefficient of the specimen. While high percentage of Cu lead to low thermal expansion coefficient of the specimen. NZ have higher microhardness than TMAZ, HAZ and the BMs which indicated presence of brittle IMCs and grain refinement. Regarding the tensile strength results, the weakest part is generally the Al side (TMAZ and NZ). The lower tensile strength is due to the formation of intermediate compounds. Finally we concluded that the friction temperature produced from rotational speed 1000rpm is considered perfect welds with acceptable mechanical properties.

Acknowledgements

This work was supported under the College of Engineering, Al-Qadisiyah University, Al-Qadisiyah, Iraq. The authors express their gratitude for the outstanding support provided by the staff at the College of Materials Engineering (UniMAP) and Universiti Teknologi Malaysia 81310 Skudai, Johor, Malaysia..

References

- [1] H. Dawood, K.S. Mohammed, A. Rahmat, M. Uday, Microstructural characterizations and mechanical properties in friction stir welding technique of dissimilar (Al-Cu) sheets, *Journal of Applied Science and Agriculture* 10(5) (2015) 149-158.
- [2] T. Lienert, R. Mishra, M. Mahoney, Friction stir welding and processing, ASM International: Materials Park, OH, USA (2007) 123-154.
- [3] S. Señorís-Puentes, R.F. Serrano, G. González-Doncel, J.H. Hattel, O.V. Mishin, Microstructure and Mechanical Properties of Friction Stir Welded AA6061/AA6061+ 40 vol% SiC Plates, *Metals* 11(2) (2021) 206.
- [4] S. Celik, R. Cakir, Effect of friction stir welding parameters on the mechanical and microstructure properties of the Al-Cu butt joint, *Metals* 6(6) (2016) 133.
- [5] K. Li, F. Jarrar, J. Sheikh-Ahmad, F. Ozturk, Using coupled Eulerian Lagrangian formulation for accurate modeling of the friction stir welding process, *Procedia Engineering* 207 (2017) 574-579.
- [6] B. Bobbs, M. Wiedmann, M. Klein, In-Line Inspection of Friction Stir Welds Using Laser Ultrasonics, *NDE of Aerospace Materials & Structures* 2018, 2018, pp. 22-31.
- [7] R. Rai, A. De, H. Bhadeshia, T. DebRoy, friction stir welding tools, *Science and Technology of welding and Joining* 16(4) (2011) 325-342.
- [8] A. Chauhan, An overview of friction stir welding process and parameters of aluminium alloys, *Research Journal of Engineering and Technology* 8(4) (2017) 306-310.
- [9] C.M.P. Maborang, J.N.B. Padriago, G.M. Quiachon, P.A.N. de Yro, Synthesis and Characterization of Electrospun Carbon Quantum Dots-Polyacrylonitrile/Polycaprolactone Composite Nanofiber Membranes for Copper (II) Adsorption, *Key Engineering Materials, Trans Tech Publ*, 2021, pp. 3-8.
- [10] Y. Hwang, P. Fan, C. Lin, Experimental study on Friction Stir Welding of copper metals, *Journal of materials processing technology* 210(12) (2010) 1667-1672.
- [11] M.F.X. Muthu, V. Jayabalan, Tool travel speed effects on the microstructure of friction stir welded aluminum-copper joints, *Journal of Materials Processing Technology* 217 (2015) 105-113.
- [12] M.P. Mubiayi, E.T. Akinlabi, Friction stir welding of dissimilar materials between aluminium alloys and copper, An overview, *Proceedings of the World Congress on*

- Engineering, IAENG Publications San Francisco, USA, 2013, pp. 3-5.
- [13] I. Galvão, D. Verdera, D. Gesto, A. Loureiro, D. Rodrigues, Influence of aluminium alloy type on dissimilar friction stir lap welding of aluminium to copper, *Journal of Materials Processing Technology* 213(11) (2013) 1920-1928.
- [14] T. Saeid, A.a. Abdollah-Zadeh, B. Sazgari, Weldability and mechanical properties of dissimilar aluminum-copper lap joints made by friction stir welding, *Journal of Alloys and Compounds* 490(1-2) (2010) 652-655.
- [15] A. Scialpi, L. De Filippis, P. Cavaliere, Influence of shoulder geometry on microstructure and mechanical properties of friction stir welded 6082 aluminium alloy, *Materials & design* 28(4) (2007) 1124-1129.
- [16] S.R. Prasad, A. Kumar, C.S. Reddy, L.S. Raju, Influence of tool shoulder geometry on microstructure and mechanical properties of friction stir welded 2014-T6 Aluminium Alloy, *Materials Today: Proceedings* 4(9) (2017) 10207-10211.
- [17] P. Xue, D. Ni, D. Wang, B. Xiao, Z. Ma, Effect of friction stir welding parameters on the microstructure and mechanical properties of the dissimilar Al-Cu joints, *Materials science and engineering: A* 528(13-14) (2011) 4683-4689.
- [18] N. Sharma, A.N. SIDDIQUEE, Friction stir welding of aluminum to copper—an overview, *Transactions of Nonferrous Metals Society of China* 27(10) (2017) 2113-2136.
- [19] T. Watanabe, H. Takayama, A. Yanagisawa, Joining of aluminum alloy to steel by friction stir welding, *Journal of Materials Processing Technology* 178(1-3) (2006) 342-349.
- [20] R.K. Shukla, P.K. Shah, Comparative study of friction stir welding and tungsten inert gas welding process, *Indian Journal of Science and Technology* 3(6) (2010) 667-671.
- [21] N.A. Muhammad, C. Wu, Ultrasonic vibration assisted friction stir welding of aluminium alloy and pure copper, *Journal of Manufacturing Processes* 39 (2019) 114-127.
- [22] S. Singh, M. MAHMEEN, Effect of tool pin offset on the mechanical properties of dissimilar materials based on friction stir welding (FSW), *Journal. International Journal of Modern Trends in Engineering and Research* 3 (2016) 75-80.
- [23] D. Lohwasser, Z. Chen, Friction stir welding: From basics to applications, Elsevier 2009.
- [24] M. Uday, M. Ahmad-Fauzi, Joint properties of friction welded 6061 aluminum alloy/YSZ-alumina composite at low rotational speed, *Materials & Design* 59 (2014) 76-83.
- [25] H. Dawood, K.S. Mohammed, A. Rahmat, M. Uday, Microstructural Characterizations and Mechanical Properties in Friction Stir Welding Technique of Dissimilar (Al-Cu) Sheets, *J. Appl. Sci. Agric* 10 (2015) 149.
- [26] M. Uday, A. Fauzi, H. Zuhailawati, A. Ismail, Effect of welding speed on mechanical strength of friction welded joint of YSZ-alumina composite and 6061 aluminum alloy, *Materials Science and Engineering: A* 528(13) (2011) 4753-4760.
- [27] A. Abdollah-Zadeh, T. Saeid, B. Sazgari, Microstructural and mechanical properties of friction stir welded aluminum/copper lap joints, *Journal of alloys and Compounds* 460(1-2) (2008) 535-538.
- [28] M. Paidar, O.O. Ojo, A. Moghanian, A.S. Karapuzha, A. Heidarzadeh, Modified friction stir clinching with protuberance-keyhole levelling: A process for production of welds with high strength, *Journal of Manufacturing Processes* 41 (2019) 177-187.
- [29] P. Bahemmat, A. Rahbari, M. Haghpanahi, M. Besharati, Experimental study on the effect of rotational speed and tool pin profile on aa2024 aluminium friction stir welded butt joints, *Proceedings of ECTC*, 2008, pp. 3-4.
- [30] H. Dawood, K.S. Mohammed, A. Rahmat, M. Uday, Effect of small tool pin profiles on microstructures and mechanical properties of 6061 aluminum alloy by friction stir welding, *Transactions of Nonferrous Metals Society of China* 25(9) (2015) 2856-2865.
- [31] O. Gopkalo, X. Liu, F. Long, M. Booth, A. Gerlich, B. Diak, Non-isothermal thermal cycle process model for predicting post-weld hardness in friction stir welding of dissimilar age-hardenable aluminum alloys, *Materials Science and Engineering: A* 754 (2019) 205-215.
- [32] H.I. Dawood, K.S. Mohammed, A. Rahmat, M. Uday, The influence of the surface roughness on the microstructures and mechanical properties of 6061 aluminium alloy using friction stir welding, *Surface and Coatings Technology* 270 (2015) 272-283.
- [33] H. Barekatin, M. Kazeminezhad, A. Kokabi, Microstructure and Mechanical Properties in Dissimilar Butt Friction Stir Welding of Severely Plastic Deformed Aluminum AA 1050 and Commercially Pure Copper Sheets, *Journal of Materials Science & Technology* (2013).
- [34] H.A. Derazkola, F. Khodabakhshi, Intermetallic compounds (IMCs) formation during dissimilar friction-stir welding of AA5005 aluminum alloy to St-52 steel: numerical modeling and

- experimental study, *The International Journal of Advanced Manufacturing Technology* 100(9-12) (2019) 2401-2422.
- [35] L. Murr, A review of FSW research on dissimilar metal and alloy systems, *Journal of materials engineering and performance* 19(8) (2010) 1071-1089.
- [36] T. Wang, H. Sidhar, R.S. Mishra, Y. Hovanski, P. Upadhyay, B. Carlson, Effect of hook characteristics on the fracture behaviour of dissimilar friction stir welded aluminium alloy and mild steel sheets, *Science and Technology of Welding and Joining* 24(2) (2019) 178-184.
- [37] H.I. Dawood, K.S. Mohammed, M.Y. Rajab, Advantages of the green solid state FSW over the conventional GMAW process, *Advances in Materials Science and Engineering* 2014 (2014).
- [38] M.R. Mohammad Aliha, Y. Fotouhi, F. Berto, Experimental notched fracture resistance study for the interface of Al-Cu bimetal joints welded by friction stir welding, *Proceedings of the Institution of Mechanical Engineers, Part B: Journal of Engineering Manufacture* 232(12) (2018) 2192-2200.
- [39] L. Fu, L. Duan, S. Du, Numerical simulation of inertia friction welding process by finite element method, *WELDING JOURNAL-NEW YORK-* 82(3) (2003) 65-S.
- [40] X.-w. LI, D.-t. ZHANG, C. QIU, W. ZHANG, Microstructure and mechanical properties of dissimilar pure copper/1350 aluminum alloy butt joints by friction stir welding, *Transactions of Nonferrous Metals Society of China* 22(6) (2012) 1298-1306.
- [41] J. Ouyang, E. Yarrapareddy, R. Kovacevic, Microstructural evolution in the friction stir welded 6061 aluminum alloy (T6-temper condition) to copper, *Journal of Materials Processing Technology* 172(1) (2006) 110-122.
- [42] X. Peng, R. Wuhler, G. Heness, W. Yeung, On the interface development and fracture behaviour of roll bonded copper/aluminium metal laminates, *Journal of materials science* 34(9) (1999) 2029-2038.
- [43] H. Jiang, J. Dai, H. Tong, B. Ding, Q. Song, Z. Hu, Interfacial reactions on annealing Cu/Al multilayer thin films, *Journal of applied physics* 74(10) (1993) 6165-6169.
- [44] M. Uday, A. Fauzi, Z. Hussain, A. Ismail, Effect of Deformation Behavior on the Grain Size of the 6061 Aluminum Alloy Joint with Alumina by Friction Welding, *Applied Mechanics and Materials* 83 (2011) 97-103.
- [45] X.-w. Li, D.-t. Zhang, Q. Cheng, W. Zhang, Microstructure and mechanical properties of dissimilar pure copper/1350 aluminum alloy butt joints by friction stir welding, *Transactions of Nonferrous Metals Society of China* 22(6) (2012) 1298-1306.
- [46] T. Hirata, T. Oguri, H. Hagino, T. Tanaka, S.W. Chung, Y. Takigawa, K. Higashi, Influence of friction stir welding parameters on grain size and formability in 5083 aluminum alloy, *Materials Science and Engineering: A* 456(1) (2007) 344-349.
- [47] P. Tayebi, A. Fazli, P. Asadi, M. Soltanpour, Formability analysis of dissimilar friction stir welded AA 6061 and AA 5083 blanks by SPIF process, *CIRP Journal of Manufacturing Science and Technology* (2019).
- [48] L. Yu, K. Nakata, J. Liao, Microstructural modification and mechanical property improvement in friction stir zone of thixo-molded AE42 Mg alloy, *Journal of Alloys and Compounds* 480(2) (2009) 340-346.
- [49] X. Xu, X. Yang, G. Zhou, J. Tong, Microstructures and fatigue properties of friction stir lap welds in aluminum alloy AA6061-T6, *Materials & Design* 35 (2012) 175-183.